Progress in Superconductivity Vol.8 No.1 pp. 81-86 31 October 2006

Resistance Development in Au/YBCO Thin Film Meander Lines under High-Power Fault Conditions

H.-R. Kim[*,a], J. Sim[b], I.-J. Choi[a], S.-W. Yim[a], O.-B. Hyun[a]

[a] *Korea Electric Power Research Institute, Daejeon, Korea*

[b] *Korea University, Seoul, Korea*

Received 16 August 2004

과도 사고 시 Au/YBCO 박막 곡선의 저항 거동

김혜림[*,a], 심정욱[b], 최인지[a], 임성우[a], 현옥배[a]

Abstract

We investigated resistance development in Au/$YBa_2Cu_3O_7$ (YBCO) thin film meander lines during high-power faults. The meander lines were fabricated by patterning 300 nm thick YBCO films coated with 200 nm thick gold layers into meander lines. A gold film grown on the back side of the substrate was also patterned into a meander line. The front meander line was connected to a high-power fault-test circuit and the back line to a DC power supply. Resistance of both lines was measured during the fault. They were immersed in liquid nitrogen during the experiment. Behavior of the resistance development prior to quench completion could be understood better by comparing resistance of the front meander lines with that of the back. Quench completion point could be determined clearly. Resistance and temperature at the quench completion point were not affected by applied field strength. The experimental results were analyzed quantitatively with the concept of heat transfer within the meander lines/substrate and to the surrounding liquid nitrogen. In analysis, the fault period was divided into three regions: flux-flow region, region prior to quench completion, and region after quench completion. Resistance was calculated for each region, reflecting the observation for quench completion. The calculated resistance in three regions was joined seamlessly and agreed well with data.

Keywords : quench, superconducting, fault current limiter, heat transfer

I. Introduction

The superconducting fault current limiter (SFCL) is a protection device that limits the fault current in electric power systems in a few milliseconds. For this reason there has been active research going on SFCLs [1-4].

Knowledge on quench properties of superconductors is important for the research and development of SFCLs, because quench property determines their performance. The resistance

*Corresponding author. Fax : +82 42 865 5804
e-mail : hrkim@kepri.re.kr

development in high-power faults is particularly important, because it is related to stability of SFCLs under over-voltage conditions. In this work, we investigated the resistance development in Au/$YBa_2Cu_3O_7$ (YBCO) thin film meander lines during high-power faults. The Au/YBCO meander lines are the core part of SFCLs based on YBCO thin films. Focus was placed particularly on the beginning of the fault, because the behavior at this time period determines the current limitation speed. Resistance of the meander lines was measured under high-power conditions, and the data were interpreted in terms of heat transfer within the meander lines/substrate and to the surrounding liquid nitrogen.

II. Experimental details

The samples were fabricated based on 300 nm thick YBCO films grown on sapphire substrates. The films were purchased from Theva in Germany. The critical current density of the films was around 3.0 MA/cm^2 and uniform within ±5 %. The film was coated in-situ with a 200 nm thick gold shunt layer, and patterned into a meander line by photolithography (Fig. 1(a)). A 200 nm thick gold layer was sometimes coated also on the back side of the substrate, and patterned into a meander line (Fig. 1(b)). The back Au meander line was used as a temperature sensor that measures the temperature at the back surface of the substrate. The pattern on the back side was aligned so that it matched with that on the front side.

Resistance of the Au/YBCO meander lines was measured using the circuit shown in Fig. 2. The meander line on the front side was connected to a fault simulation circuit. An AC power supply was used as the voltage source, V_o. The fault was simulated by closing a switch connected across the load, S_2, and cut off with switch S_1 several cycles after the fault so that the sample would not be subjected to fault currents for unnecessarily long time. The Au meander line on the back side was connected to a DC power suppply. The applied current was low enough for the heat generated in the Au meander line to be negligible. Voltage taps were mounted on pads along the meander lines on both the front and back sides of SFCLs to measure the resistance distribution. Voltages and currents were measured simultaneously with a multi-channel data acquisition system. During the measurement, the samples were immersed in liquid nitrogen for effective cooling.

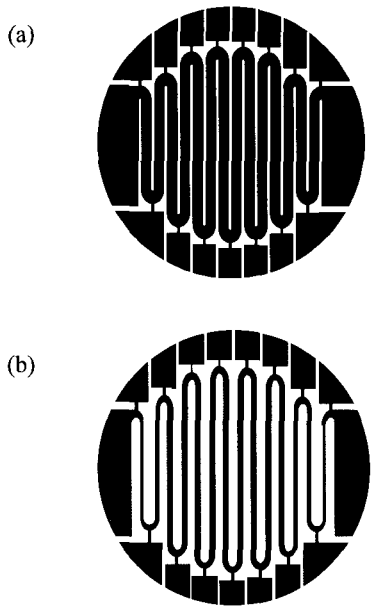

Fig. 1. The pattern of meander lines (a) on the front side, and (b) on the back side.

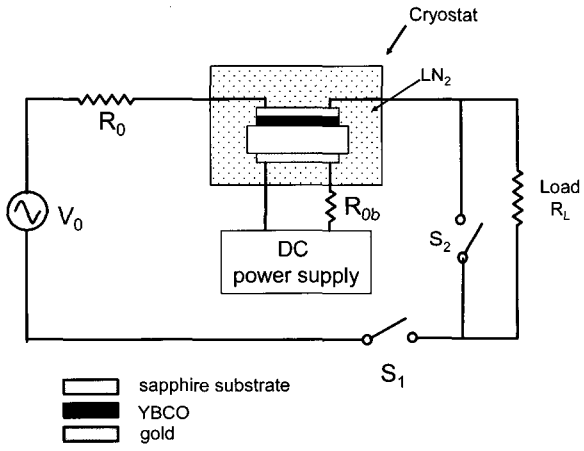

Fig. 2. The resistance measurement circuit.

III. Results and discussion

Fig. 3 shows the resistance development of the meander lines on the front and the back sides. The resistance was normalized with its room temperature value. Horizontal lines indicate temperature of the meander lines. The temperature could be estimated from the linear relation between resistance and temperature of metals. The figure shows that resistance of the front meander line increased rapidly to values higher than the resistance at 87 K, the critical temperature (T_c) of the YBCO film, in the first half cycle. Resistance of the back meander line increased more slowly to similar values. Two curves met at point B. After point B they fell more or less on top of each other, which indicates that the average temperature of the back meander line is nearly the same as that of the front. Details on this observation can be found in [5], which concluded that the average temperature of the front and the back meander lines are nearly the same due to high thermal conductivity of sapphire substrate below about 150 K. The conclusion tells that resistance of the back meander line can be used to estimate the average temperature of the front meander line below 150 K. Fig. 3 shows that the temperature increased immediately after quench started at point A, and that the resistance and the temperature increased together. As the average temperature increased, quench propagated and the resistance increased rapidly. The resistance increased fast up to point B, which is due to the superconducting-to-normal-state transition. This means that quench was completed at point B. Up to that point a part of meander line was in the superconducting state. After B, resistance increased more slowly.

Resistance development at different field strength was shown in Fig. 4. The behavior was similar except that resistance increased more slowly at lower field strength and that consequently quench was completed at later times. At 3.6 V/cm, it was completed at around 13 ms after the quench. Noteworthy is that resistance at quench completion point was all about 0.51 of room temperature value at

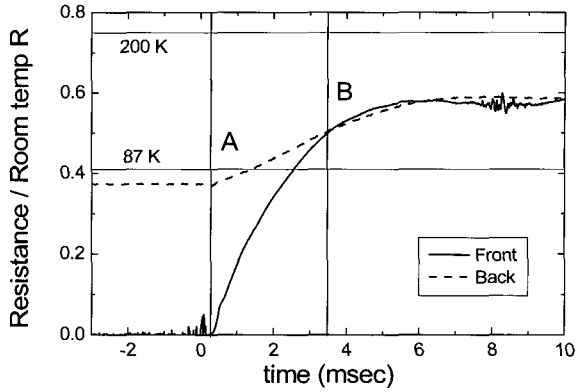

Fig. 3. Resistance of meander lines on the front and the back meander lines. Applied field strength was 6.7 V_{rms}/cm.

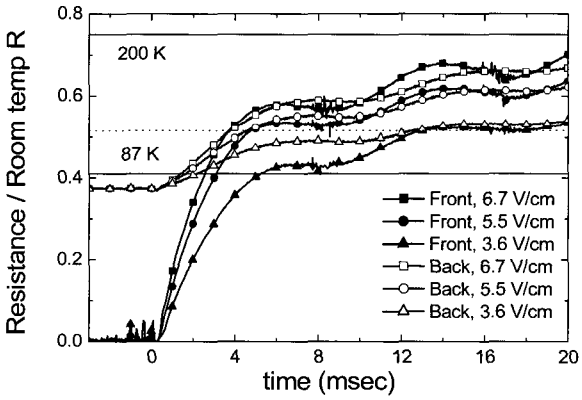

Fig. 4. Resistance of meander lines on the front and the back meander lines for selected field strength.

different field strength, which was marked with a dotted horizontal line in Fig. 4. The corresponding temperature was about 127 K.

In order to understand the above behavior better, resistance distribution was measured and shown in Fig. 5. Since it was more or less symmetric, resistance of stripes 1, 2, 5 and 7 only were shown for simplicity. Stripe 1 is the stripe next to an electrode, and stripe 7 near the center. Resistance distribution was very non-uniform at the beginning of the quench. In stripes 5 and 7 the resistance increased immediately, but in other stripes it increased 0.6~1.1 ms later. By the time the quench started in stripe 1, the resistance of stripe 7 reached about 0.3 times the

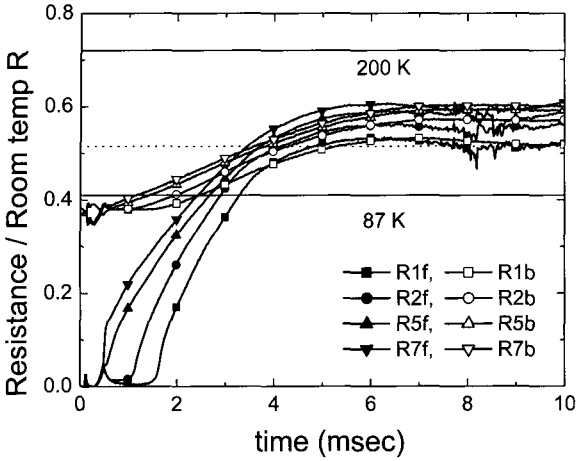

Fig. 5. Resistance of selected stripes on the front (soild marks) and the back sides (open marks). Applied field strength was 6.7 V_{rms}/cm.

room temperature value, and its average temperature was above T_c. As the time elapsed, resistance of the stripes near the electrode increased faster, and the resistance distribution became fairly uniform by the time quench was completed. Resistance at quench completion point was about 0.50 of room temperature value in all stripes. It was slightly higher at the center stripes than at the stripes near the electrode. In order to see resistance distribution more clearly, the resistance at different times after the fault is plotted as a function of position in Fig. 6. Data points from left to right (1.25 mm to 16. 25 mm from the center) correspond to resistance of stripe 7 to stripe 1. Resistance of center stripes increased rapidly at the beginning, but the increase slowed down. That of the stripes near the edge caught up soon, and the resistance distribution became uniform except at stripe 1.

Resistance development in meander lines could be quantitatively explained in terms of heat transfer within the meander lines/substrate and to the surroundings. Focus is placed here on high-power quench at the beginning of the fault, as mentioned in the introduction. When high voltages are applied across the meander lines, a large amount of Joule heat is generated after quench starts, and the quench propagates very fast. The quench is completed before

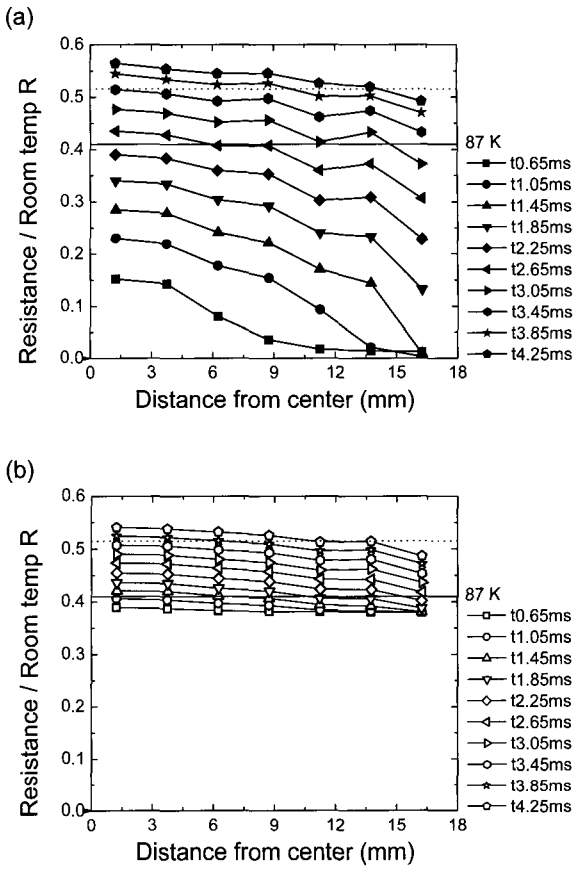

Fig. 6. Resistance distribution at (a) the front and (b) the back meander lines at selected times after the fault. Applied field strength was 6.7 V_{rms}/cm.

the current reached the first peak. In calculating the resistance, the fault period was divided into three regions, and resistance was calculated separately for each region: flux-flow region, region prior to quench completion, and region after quench completion. It is because resistance in each region is generated by different mechanisms. In the flux-flow region,

$$R=\frac{10^{-6} I}{I_c}\left(\frac{I}{I_c}\right)^{n-1}, \tag{1}$$

where l is length of the meander line. Once quench started, the resistance is generated due to the superconducting-to-normal-state transition, until the quench is completed. The resistance can be expressed

as follows [6]:

$$R = -R_0 + \left(B_p^2 + A_p \exp(-(t - t_p)/\tau_p)\right)^{1/2}$$
$$B_p^2 = R_0^2 + D_p^2 V_0^2 \quad (2)$$
$$A_p = (R(t_p) + R_0)^2 - B_p^2$$
$$D_p^2 = R_f/(\gamma\beta), \tau_p = C/(2\gamma),$$

where R_0, V_0, γ, C, t_p are the circuit resistance and voltage (See Fig. 2), heat transfer coefficient, heat capacity, time point at which quench started, respectively. R_f and β are resistance and temperature of the meander line at the quench completion point. The values mentioned above were used in the calculation. After quench completion, resistance increases due to the temperature increase of the meander line and the linear relation between resistance and temperature of metals: $R = a\,T + b$, where a and b are constants. In this region [7],

$$R = \alpha/2 + \left(B_a^2 + A_a \exp(-(t-t_a)/\tau_a)\right)^{1/2}$$
$$B_a^2 = (\alpha/2)^2 + D_a^2 V_0^2, \; A_a = (R_f - \alpha/2)^2 - B_a^2 \quad (3)$$
$$D_a^2 = a/\gamma, \; \tau_a = C/(2\gamma),$$

where α and t_a are resistance of the Au layer at liquid nitrogen temperature and time point at which quench is completed, respectively.

The calculation result for resistance of the meander line at applied field strength of 6.7 V_{rms}/cm is shown in Fig. 7, along with the data. The resistance in three regions is joined seamlessly and agrees well with data. The discrepancy is due to the oscillatory nature of AC power. The calculation here did not include the oscillatory part of the resistance.

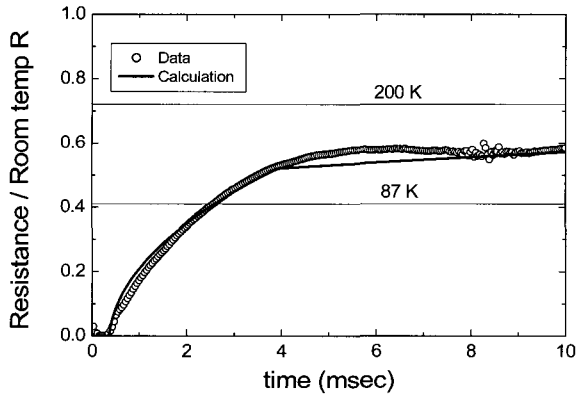

Fig. 7. Calculation result and data for resistance of the meander line at applied field strength of 6.7 V_{rms}/cm.

IV. Conclusions

We investigated resistance development in Au/YBCO thin film meander lines during high-power faults. Behavior of the resistance development prior to quench completion was understood better by comparing resistance of the front meander lines with that of the back. Quench completion point could be determined clearly. Resistance and temperature at the point was not affected by applied field strength. Experimental results were analyzed quantitatively with the concept of heat transfer within the meander lines/substrate and to the surrounding liquid nitrogen. In analysis, the fault period was divided into three regions: flux-flow region, region prior to quench completion, and region after quench completion. Resistance was calculated for each region, reflecting the observation mentioned above for the quench completion. The resistance in three regions was joined seamlessly and agreed well with data.

Acknowledgments

This research was supported by a grant from Electric Power Industry Technology Evaluation and Planning funded by the Ministry of Commerce, Industry and Energy, Republic of Korea.

References

[1] M. Chen et al., "6.4 MVA resistive fault current limiter based on Bi-2212 superconductor," Physica C, 372-376 1657-1663 (2002).

[2] Y. Kudo, H. Kubota, H. Yoshino, and Y. Wachi,

"Improvement of maximum working voltage of resistive fault current limiter using YBCO thin film and metal thin film," Physica C, 372-376, 1664-1667 (2002).

[3] J. Bock et al., "Development and successful testing of MCP BSCCO-2212 components for a 10 MVA resistive superconducting fault current limiter," Supercond. Sci. Technol. 17, S122–S126 (2004).

[4] H. P. Kraemer, W. Schmidt, H. W. Neumueller, and B. Utz, "Switching behavior of YBCO thin film conductors in resistive fault current limiters," IEEE Tr. Applied Supercond. 13, 2044-2047 (2003).

[5] Hye-Rim Kim, Jungwook Sim, Ok-Bae Hyun, "Temperature distribution in SFCLs based on Au/YBCO films during quenches", Cryogenics, 46, 305-311 (2006).

[6] Hye-Rim Kim, Ok-Bae Hyun, Hyo-Sang Choi, Sang-Do Cha, and Je-Myung Oh, "Resistance Development in Superconducting Fault Current Limiters Prior to Quench Completion," IEEE Tr. Applied Supercond. 13, 2032-2035 (2003).

[7] Hye-Rim Kim, Hyo-Sang Choi, Hae-Ryong Lim, In-Seon Kim, Ok-Bae Hyun, "Resistance of superconducting fault current limiters based on $YBa_2Cu_3O_7$ thin films after quench completion", Physica C, 372-376, 1606-1609 (2002).